Acta Geophysica (2024) 72:1097–1112
https://doi.org/10.1007/s11600-023-01075-8

RESEARCH ARTICLE - HYDROLOGY

Effects of vegetation distribution along river transects on the morphology of a gravel bed braided river

Runye Zhu[2] · **Ryota Tsubaki**[1] · **Yuji Toda**[1]

Received: 5 November 2022 / Accepted: 12 March 2023 / Published online: 4 April 2023

Abstract

The interaction between vegetation, sediment, and water flow creates various fluvial landscapes. Hydrological conditions and flood disturbances, as well as the habitat preference of vegetation, regulate its spatial distribution. To describe the spatial distribution of vegetation cover, here, we focus on vegetation distributions along river transverse transects that define vertical and horizontal distances from water areas during low flow periods. As one of the most dynamic river types, braided rivers can be significantly influenced by vegetation encroachment. However, the effects of vegetation distributions along river transects on braided river morphology remain unknown. To study the potential influence of vegetation distribution along river transects, a depth-averaged, hydro-morphodynamic model was employed. Using the model, we investigated a medium-sized, braided river with a gravel bed affected by riparian vegetation. The following scenarios of vegetation transect distributions were examined: (1) vegetation established near or covering the low water channel, and (2) vegetation established on bar tops and kept at a distance from the low water channel. The model successfully reproduced a reduction in the braiding index for a vegetated braided river. Depending on the transect distribution scenarios employed, significantly different effects for river morphology were obtained. For example, compared to vegetation on bar tops, vegetation located near the low water channel played a more critical role for changing river morphology, redirecting water flow, and changing the statistical characteristics of the riverbed elevation distribution. Vegetation near the low water channel not only concentrated water flow to low water channels but also redirected flow to the high elevation area by reducing low water channel flow capacity. The revealed effects of the vegetation transect distribution on river morphology development helped to determine effective management protocols for reducing the negative impact of vegetation encroachment.

Keywords Vegetation distribution · Braided river · River morphology · Delft3D

List of symbols

A	The coefficient used to account for the secondary flow effect (–)
a_s	The vegetation density, which is the product of stem number per unit area and the vegetation representative diameter (m^{-1})
C	The Chezy's coefficient ($m^{1/2}\ s^{-1}$)
C_D	The drag coefficient (−)
d	The sediment diameter (m)
t	Time (s)
g	Gravitational acceleration ($m\ s^{-2}$)
H	The water surface elevation (m)
h	Water depth (m)
h_v	The submerged vegetation height (m)
f	The coefficient used to account for the bed slope effect on the bedload transport direction (–)
F_x, F_y	The drag force acting on vegetation in the x and y directions, respectively (N)
R	The radius of streamline curvature (m)
u, v	The depth-averaged velocity components for the x and y directions, respectively ($m\ s^{-1}$)
V	The horizontal eddy viscosity ($m^2\ s$)
X, Y	Horizontal coordinates for the longitudinal and transverse directions, respectively (m);
z_b	The bed elevation (m)
α, β	The coefficients used in the model to account for the bed slope effect on the bedload transport direction (–)

Edited by Dr. Michael Nones (CO-EDITOR-IN-CHIEF).

✉ Ryota Tsubaki
rtsubaki@civil.nagoya-u.ac.jp

[1] Nagoya University, Nagoya, Japan

[2] Zhejiang Institute of Hydraulics and Estuary, Hangzhou, People's Republic of China

θ The Shields number (–)
κ The von Kármán's constant (–)
ρ The density of water (kg m^{-3})
ρ_s The density of sediment (kg m^{-3})
τ The bed shear stress (N m^{-2})
Φ_τ The angle between bedload transport and the depth-averaged velocity accounting for the secondary flow effect (radian)
Φ_s The angle between bedload transport on a sloped bed and the depth-averaged velocity (radian)

Introduction

Since the interaction between hydrology, sediment transport, and vegetation creates diverse river morphology and landforms (Millar 2000; Tsujimoto 1999), riparian vegetation plays an important role in river morphology (Gurnell 2014). Riparian vegetation changes river morphology because it decreases flow velocity within vegetation patches and promotes sediment deposition (Kim et al. 2015; Tsujimoto 1999; Zong and Nepf 2011). Vegetation patches also deflect water flow and induce morphological change at the area distant from vegetation (Bywater-Reyes et al. 2018). By stabilizing bar tops and blocking side channels, uniformly and widely distributed vegetation has the potential to transform a braided river into a single-thread river (Gran and Paola 2001; Tal and Paola 2007). In nature, the spatial distribution of vegetation differs depending on vegetation species and the environment (e.g., flow disturbance and water availability). The vegetation distribution within a river transverse transect has different patterns. For example, some pioneer species prefer habitat near the water's edge during low discharge periods. Meanwhile, others prefer bar tops where the flow disturbance is relatively minor. Due to the keen scale effect, reproducing such vegetation distribution patterns in laboratory experiments is difficult. Although many previous studies have investigated the effect of the vegetation distribution in single-thread rivers, the effects of the vegetation distribution on braided rivers are rarely investigated. Along a braided river transverse transect, vegetation, depending on its vertical location relative to the water's surface, may interact, at different degrees, with river morphology (Gurnell 2014). Nevertheless, how differences in the vegetation distribution affect river morphology development remains unclear. In this study, we examined the effect of the vegetation distribution in a river transverse transect on braided river morphology.

The vegetation spatial distribution is determined by several factors, such as vegetation species, hydrological conditions, and climate conditions (Camporeale and Ridolfi 2006; Gurnell 2014; Vargas-Luna et al. 2019). Vegetation may colonize a stable river bed where the underground water stage enables its growth (Mahoney and Rood 1998). Discharge variability, which induces flood disturbances and changes water availability during low flow periods, is an important factor that impacts the vegetation distribution within transects (Camporeale and Ridolfi 2006). The distribution of vegetation along a transect direction is also affected by the process of vegetation seed dispersal (Van Dijk et al. 2013). Furthermore, artificial impacts on rivers (e.g., dam construction) may also lead to a change in the spatial distribution of vegetation (van Oorschot et al. 2018). Depending on propagule stress, alien vegetation invasion can significantly change the spatial distribution of vegetation (van Oorschot et al. 2017). Climate change may also induce vegetation belt shifting and changes in species richness; and depending on changes in hydrological conditions and the vegetation distribution, the vegetation belt may shrink or expand (Martínez-Fernández et al. 2018; Mosner et al. 2015; Ström et al. 2012).

The vegetation spatial distribution makes river morphology distinct from areas without riparian vegetation. An early numerical study indicated that the non-uniform vegetation distribution on a floodplain influenced the planform of meandering rivers (Camporeale et al. 2013). The distribution of vegetation in the transverse direction also has an impact on rivers with alternate bars (Bertoldi et al. 2014). In single-thread rivers, vegetation surrounding water edges and vegetation on bar surfaces have different effects on river morphological change (Vargas-Luna et al. 2019). Vegetation surrounding water edges makes the riverbank more stable, while vegetation on a bar surface alters the river flow direction and induces local bank erosion. A river with vegetation whose seeds are transported by water flow tends to have a larger braiding intensity as compared to a river with vegetation whose seeds are transported by wind (Van Dijk et al. 2013). In a field study performed within the Tagliamento River in Italy, researchers found that the statistical properties (i.e., the variance, skewness, and kurtosis of the river bed elevation distribution) of an island braiding river are related to the median elevation of the vegetation patch (Bertoldi et al. 2011), suggesting that river morphology development may be related to the vegetation distribution. The bed elevation distribution was also found to be negatively skewed, and skewness was positively related to the vegetation area ratio increase. However, in a flume experiment performed by Mao et al. (2020), skewness of the bed elevation distribution decreased with vegetation encroachment on bar surfaces.

Due to the difficulty in controlling vegetation distributions while keeping the physical properties of vegetation constant, studying the effects of different vegetation distributions along transects on river morphology development via laboratory experiments is difficult. Recently, sophisticated, depth-averaged, two-dimensional numerical models have been shown to reproduce the morphological development

of rivers with vegetation (Jourdain et al. 2020; van Oorschot et al. 2016; Weisscher et al. 2019). In our study, numerical simulations based on Delft3D were performed in order to study the effect of differences in the vegetation distribution along transects on braided river morphological development and the statistical properties of river morphology. We investigated two different vegetation colonization types within a gravel bed, braided river. The first colonization type accounted for vegetation colonizing near water edges during the low discharge period. For the second type of colonization, vegetation colonized from a higher elevation where flow disturbances were relatively weak. We also compared morphology property changes due to two vegetation colonization types. Our river was inspired by the Satsunai River and the Otofuke River, two rivers which flow in Hokkaido, Japan that have been heavily influenced, over the past decade, by vegetation (Iwasaki et al. 2016a; Weisscher et al. 2019). For our study, river configurations were typically gravel bed rivers sensitive to vegetation expansion (Millar 2005).

Methods

In our study, hydro-morphology and vegetation models were alternately performed. The simulation strategy is shown in Fig. 1. The results obtained from the hydro-morphological model were used to update the vegetation model, and results of the vegetation model were transferred to the hydro-morphological model. This process has been successfully applied in early numerical simulations (van Oorschot et al. 2016).

The hydro-morphological model

Hydro-morphological development was simulated using the hydro-morphological model Delft3D. Details regarding the numerical method can be found in Lesser et al. (2004). The model solves a set of depth-averaged, shallow water equations using the Alternating Direction Implicit (ADI) method discretized into a boundary fitting grid, and then updates bed topography by solving the Exner equation.

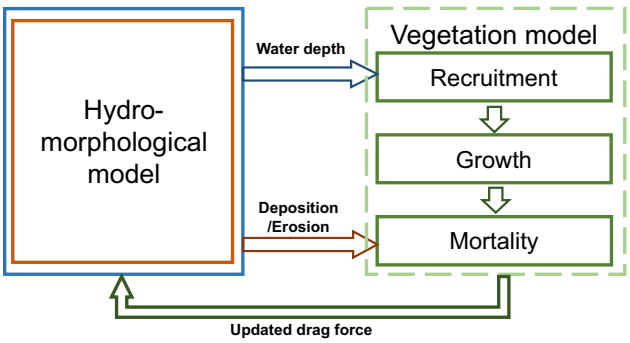

Fig. 1 Framework of the simulation model

Vegetation effects on flow are accounted for by adding source terms representing the drag force exerted on water flow, based on the following momentum equations (Jang and Shimizu 2007):

$$F_x = \frac{1}{2} C_D a_s h_v u \sqrt{u^2 + v^2}, \tag{1}$$

and

$$F_y = \frac{1}{2} C_D a_s h_v v \sqrt{u^2 + v^2}, \tag{2}$$

where x is the longitudinal coordinate, y is the transverse coordinate, u is velocity along the x direction, v is velocity along the y direction, C_D is the drag coefficient, a_s is the vegetation density that is the product of stem number per unit area and the vegetation representative diameter, and h_v is the submerged vegetation height, where the smallest value for water depth and total vegetation height is utilized.

The momentum equations are, as follows:

$$\frac{\partial u}{\partial t} + u\frac{\partial u}{\partial x} + v\frac{\partial u}{\partial y} + g\frac{u\sqrt{u^2+v^2}}{C^2 h} - V\left(\frac{\partial^2 u}{\partial x^2} + \frac{\partial^2 u}{\partial y^2}\right) + F_x = 0, \tag{3}$$

and

$$\frac{\partial v}{\partial t} + u\frac{\partial v}{\partial x} + v\frac{\partial v}{\partial y} + g\frac{v\sqrt{u^2+v^2}}{C^2 h} - V\left(\frac{\partial^2 v}{\partial x^2} + \frac{\partial^2 v}{\partial y^2}\right) + F_y = 0, \tag{4}$$

where H is the water surface elevation, h is water depth, g is gravitational acceleration, C is the Chezy coefficient, V is the horizontal eddy viscosity, and, as defined in Equations and, respectively, F_x and F_y are the flow resistance induced by vegetation.

Bedload flux is estimated using the Meyer-Peter and Mueller formula with a uniform grain size assumption (Colombini et al. 1987). The direction of bedload flux relative to the mean flow direction is corrected by considering the secondary flow effect and the bed slope effect. The secondary flow effect is induced by flow curvature and is critical for the formation of channel bars (Iwasaki et al. 2016b; Schuurman et al. 2013). The angle between bedload transport and the mean flow direction was calculated using:

$$\tan\left(\phi_\tau\right) = \frac{v}{u} - A\frac{h}{R}, \tag{5}$$

and

$$A = \frac{2}{\kappa^2}\left(1 - \frac{\sqrt{g}}{\kappa C}\right), \tag{6}$$

where R is the radius of the streamline curvature and κ is the von Kármán's constant that is equal to 0.4.

The effect of bed slope on bedload transport is accounted for using the following formulas:

$$\tan\left(\phi_s\right) = \frac{\sin\left(\phi_\tau\right) + f(\theta)\frac{\partial z_b}{\partial y}}{\cos\left(\phi_\tau\right) + f(\theta)\frac{\partial z_b}{\partial x}}, \tag{7}$$

and

$$f(\theta) = \frac{1}{\alpha\theta^\beta}, \tag{8}$$

and

$$\theta = \frac{\tau}{\left(\rho_s - \rho\right)gd}, \tag{9}$$

where ϕ_s is the angle between bedload flux and the mean flow direction accounting for the bed slope effect, θ is the Shields number, τ is the bed shear stress, ρ_s is the sediment density, ρ is the water density, and d is the sediment diameter. The bed slope effect is critical for braided river morphology simulations. The selection of parameter α significantly affects braiding morphology; a physically validated value of 0.7 was used in our study (Baar et al. 2019; Schuurman et al. 2018, 2013).

The vegetation model

The vegetation model was performed after the hydro-morphological model (Fig. 1). In general, the vegetation model consists of the recruitment, growth, and mortality of vegetation (Camporeale et al. 2013; Solari et al. 2016; van Oorschot et al. 2016). Recruitment occurs during the vegetation seed dispersal period and converts bare grids that meet certain criteria to vegetated grids. Vegetation growth indicates the change of vegetation characteristics (e.g., stem density, height and root depth), with time, and can be described using different functions. The mortality of vegetation included in the model represents two processes: vegetation washout induced by erosion and its burial induced by sedimentation.

For our study, we considered a simplified hydrograph, which consisted of a series of floods connected by the low discharge period. We assumed that vegetation disperses its seeds during the low discharge period. During the seed dispersal period, vegetation establishes its community on a bare bed, where the water depth is smaller than a threshold value (e.g., the dry–wet criteria of the Delft3d model). Once vegetation is established within a grid, the grid is regarded as vegetated and cannot be recolonized until vegetation is destroyed by flood disturbances (i.e., through washout or burial). We considered vegetation characteristics including vegetation height, density, and root depth.

The model tracks the cumulative bed elevation change in vegetated grids. When the cumulative scour depth within a vegetation grid becomes deeper than root depth during a flood, vegetation is assumed to be washed out (Edmaier et al. 2015). Vegetation burial occurs when the cumulative bed elevation aggradation surpasses vegetation height. The model resets and stops tracking the cumulative bed elevation change in grids where flood disturbance destroys vegetation and resumes when vegetation recolonizes. In bare grids, the additional drag induced by vegetation is zero.

In this study, the stem number per area of vegetation was 40 m^{-2} and the stem diameter was 0.005 m. The root depth was 0.3 m. Although vegetation characteristics were based on a reed grass plant, *Phragmites japonica*, we did not seek to reproduce a prototype in the field or to study the influence of specific vegetation. Vegetation parameters were configured based on the range of physical vegetation properties (Crosato and Saleh 2011; Sumi et al. 2003; van Oorschot et al. 2017; Vargas-Luna et al. 2016). Due to the relative high growth rate of grass plants (Kang et al. 2002), the growth process of vegetation during the low discharge period was neglected (i.e., vegetation was mature once it was established on riverbeds). Accordingly, the height of vegetation was set at 2.5 m during each recruitment and growth period. The parameters are summarized in Table 1.

Simulation scenarios and parameters

The target river was a medium-sized, gravel bed river with a braided morphology. The river did not represent a real river in nature, but settings for the simulated river had similar characteristics, including for slope and peak discharge, to the Satsunai River in Japan, a typical gravel bed river. The width of the river in our study was 250 m, and the channel length was 4000 m. There were 50 and 400 grids in the transverse and longitudinal direction, respectively. The river slope was set to 1/130. The gravel size was 25 mm. The Chezy roughness of the bare bed was set to 30 $m^{1/2}\ s^{-1}$. The equilibrium condition was used for the sediment inlet. The initial bed

Table 1 Vegetation parameters

Item	Unit	Value
Stem number per unit area, d	m^{-2}	40
Stem diameter	m	0.005
Stem height	m	2.5
Root depth	m	0.3
Drag coefficient, C_D	–	1.0

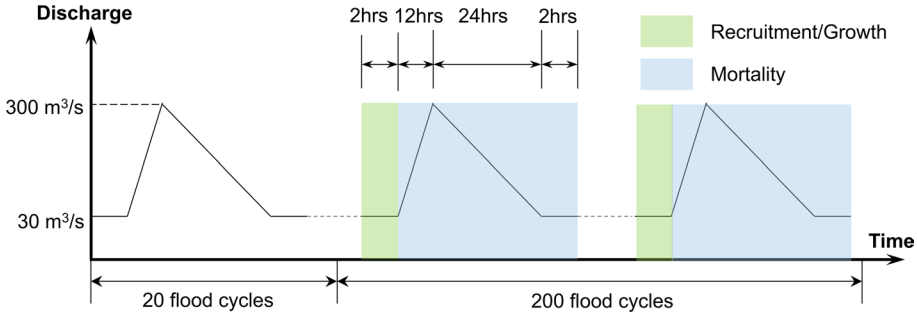

Fig. 2 A schematic of a simulation hydrograph. During the period marked by the green color, vegetation recruitment and growth were applied. During the period marked by a blue color, vegetation mortality induced by washout and burial were applied

was flat, with random elevation disturbances equal to the sediment diameter.

The entire simulation contained 220 cycles of floods and low flow. A schematic is provided in Fig. 2. A flood was assumed to occur once per year. Due to relatively minor morphological changes, the low discharge period was shortened. During the first 20 flood cycles, to develop an initial braided river morphology, the domain kept no vegetation. Once initial braiding developed, vegetation began to colonize and was recruited onto the riverbed during low flow periods (in Fig. 2 the recruitment period is marked green). Each cycle of flooding contained a 12-h rising phase and a 24-h falling phase. Before and after a flood, there were 2 h of a low discharge period. The total simulation duration of 220 cycles of floods was enough for the morphology to reach a dynamic equilibrium state where the change of bed elevation became gentle. Each flood had a typical duration for a mountainous region. Maximum discharge was 300 m^3/s, which matched the average peak of the Satsunai River in Japan (Nagata et al. 2016). Related parameters for the numerical simulation are summarized in Table 2.

Two scenarios of vegetation distribution along the transverse cross section of the river were investigated. Figure 3a and b compares the vegetation distribution of two scenarios, along the averaged cross section of a braided river, for simplicity, schematically illustrated as a single channel. In Scenario 1 (Fig. 3a), vegetation established from the water's edge to a specific upper limit of relative height, R_{UL}, during the low water period, represented vegetation species preferring moist soil (e.g., *Phragmites japonica*). In Scenario 2 (Fig. 3b), vegetation was established from the bar top to the lower limit of colonization, R_{LL}, representing vegetation that prefers a relatively dry area and avoids water edges where they are the subject of frequent flow disturbances. Several ecological processes (e.g., alien vegetation invasion, vegetation expansion, or vegetation succession) can induce a change in the upper limit R_{UL} (or the lower limit R_{LL}). A change in the upper limit (or lower limit) of the vegetation belt changes the vegetation cover area, and river morphology accordingly adjusts. For each scenario, several cases having a different R_{UL} or R_{LL} were simulated in order to investigate the sensitivity of river morphology to a change in the vegetation cover area. Table 3 presents the R_{UL} and R_{LL} values used in this study. Since our focus was on the implication of the vegetation distribution on morphological changes, and since why and how vegetation distributions

Table 2 Settings for the numerical simulation

Item	Unit	Value	Reference
Channel width	m	250	An estimation based on the field
Channel length	m	4,000	More than 10 times the channel width
Channel slope	–	1/130	Nagata et al. (2016)
Bed gravel size, d	m	0.025	Iwasaki et al. (2016a)
Maximum discharge	m^3/s	300	Nagata et al. (2016)
Mean annual low flow (vegetation recruitment)	m^3/s	30	Nagata et al. (2016)
Chezy roughness	$m^{1/2}\ s^{-1}$	30	–
Sediment inlet	–	Equilibrium condition	–
Sediment transport	–	Bedload	Determined by the Shields stress and the sediment diameter
Bed slope effect,α	–	0.7	Based on Baar et al. (2019) and Schuurman and Kleinhans (2015)
Grid size	m^2	5×10	A balance between precision and computational resources
Time step	s	0.6	Kept the simulation stable

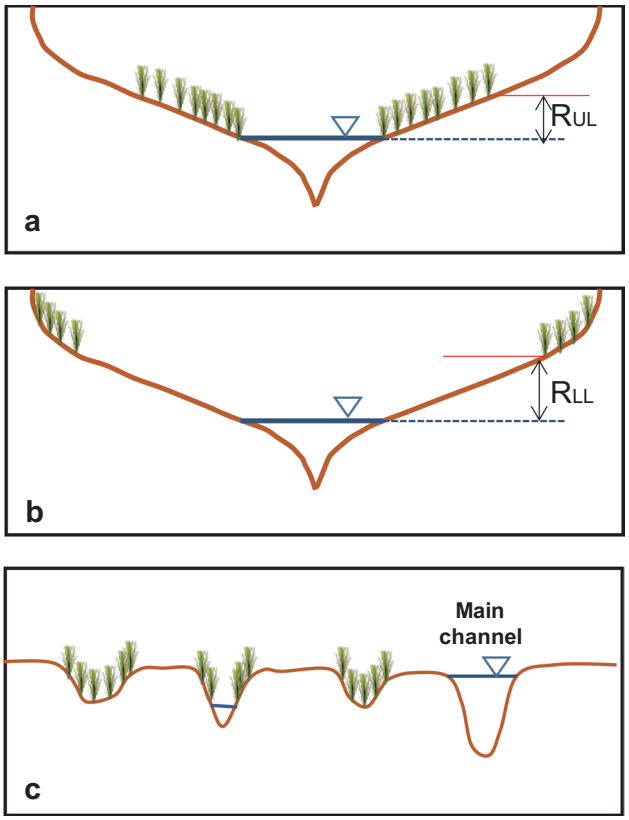

Fig. 3 Schematics of two scenarios for the vegetation distribution along averaged river transects (the brown lines) of a braided river during the low flow period (water level is indicated with blue lines) represented, for simplicity, as a single channel ((**a**) and (**b**) for Scenario 1 and Scenario 2, respectively); and the vegetation distribution along a river transect with a main channel and smaller channels (cover of the dry area below the water level of the main channel during low flow (**c**))

Table 3 The values of R_{UL} and R_{LL} studied in the simulation

	Item	Values (m)
Upper limit of Scenario 1	R_{UL}	0, 0.2, 0.5, 1.0, and 1.5
Lower limit of Scenario 2	R_{LL}	0, 0.2, 0.5, 0.7, and 1.0

change was not our focus, the transitional process was not further investigated. In addition to these two scenarios, two reference cases, including a case where vegetation covered all dry areas (referred to as the "full" case) and a case without vegetation (referred to as the "bare" case), were also simulated. The full cover case corresponded to a situation where R_{UL} was equal to the highest elevation of each cross section or where R_{LL} was equal to the lowest elevation at each cross section. Similarly, the bare case corresponded to a situation where R_{UL} was equal to the lowest elevation of each cross section or where R_{LL} was equal to the highest elevation at each cross section.

Figure 3a and b explains the situation for an averaged cross section. However, the braided river consisted of multiple channels and careful consideration of such factors was required in order to model vegetation cover. To determine relative height, the water surface elevation of the main channel during the vegetation recruitment period was used as datum. A channel with a water depth larger than the average water depth during a low flow period was regarded as the main channel. Flume experiments indicate that vegetation in braiding branches and near water edges play an important role in changing river morphology (Tal and Paola 2010). As shown in Fig. 3c, in Scenario 1, vegetation was capable of growing in low places when vegetation covered a dry area that had a relative height lower than 0 m.

Data analysis

By subtracting the mean longitudinal slope from the bed elevation, the effect of slope was excluded and the detrended bed elevation was obtained. Data employed for further analysis included results obtained once the simulation reached a state of dynamic equilibrium. Here, the dynamic equilibrium state was determined once the 5th (P5) and 95th (P95) percentile values of the detrended bed elevation stopped continuously decreasing or increasing (i.e., the riverbed was in a relatively stable state). In our study, the bed elevation of the low discharge period for the last 100 cycles of flooding was used for the analysis. To ascertain the effect of vegetation distribution along river transects, the following quantities were calculated using extracted data. For the simulation, the wet area indicated an area with a water depth larger than 0.1 m. Averaged water depth and width were estimated based on this wet area. The braiding index (BI) is the average channel number within a river cross section, and channels with a lower elevation than the averaged elevation were counted at each cross section (Schuurman and Kleinhans 2015). The interval of each cross section was 10 m. The active channel width indicates the width of channels with bedload transport. The active braiding index (ABI) is the number of channels with bedload transport when the hydrograph reaches maximum discharge. Statistical characteristics of the bed elevation distribution (i.e., variance, skewness, and kurtosis) were calculated using the slope-detrended bed elevation. The vegetation area ratio in the following figures indicates the ratio of vegetation cover area relative to the entire domain at the time just after vegetation colonization. A simulation with three slightly different initial bed disturbances was performed, and, to mitigate the dependence of initial conditions on the obtained results, the average of three implementations are indicated.

Results

River morphology

Figure 4 provides the river morphology and vegetation distribution of four representative cases. For the bare case (shown at the top of Fig. 4), the river displayed a braided feature. In Scenario 1, with $R_{UL}=0.2$ m (the second row of Fig. 4), the main channel deepened and vegetation covered water edges and low areas on the riverbed. In Scenario 2, with $R_{LL}=0.2$ m (the third row of Fig. 4), the main channel was eroded more than the main channel in Scenario 1, and vegetation covered bar tops. Compared to Scenario 1, the main channel of Scenario 2 was less affected by vegetation. For the full cover case (shown at the bottom of Fig. 4), one main channel formed and the remaining areas were vegetated bars. Compared to other cases, the patch persistence period of vegetation for the fully covered case was the highest, indicating that vegetation habitat was stable.

The P5 and P95 values for detrended bed elevation relative to the vegetation area ratio are provided in Fig. 5. Here, P5 corresponds to the bed elevation of the main channel and P95 corresponds to elevation of the bar top. Vegetation area ratio changes depended on the value of R_{UL} and R_{LL} (the values are listed in Table 3) As shown in Fig. 3, with an increase of R_{UL} and a decrease of R_{LL}, the vegetation area ratio increased. To compare the P5 and P95 of a similar vegetation area for two scenarios, the vegetation area ratio was selected for the horizontal axis of Fig. 5. For Scenarios 1 (red circles) and 2 (blue circles), since the sediment was gravel and since the simulated flood discharge was not large enough to heighten the elevation of bar tops, the P95 elevation (upper circles) did not significantly change when the vegetation area ratio increased. However, in Scenario 1 (lower red circles), the P5 value significantly decreased with an increase in the vegetation area ratio. In Scenario 2, the P5 elevation (lower blue circles) did not substantially change with an increase in the vegetation area ratio. However, if vegetation is capable of expanding near the main channel, the P5 value may rapidly decrease to approach P5 for the full cover case (the right bottom filled circle). The result for P5 in Scenario 2 indicates that vegetation located within higher elevations does not deepen the main channel.

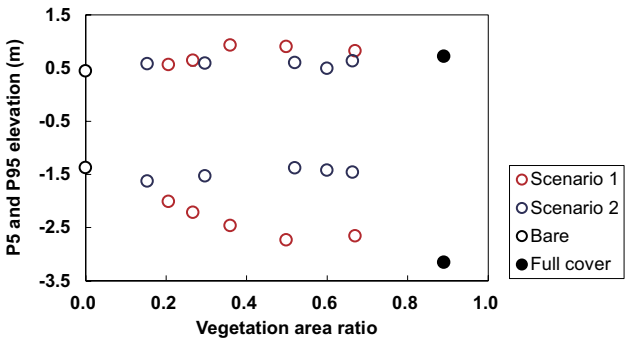

Fig. 5 P5 and P95 values for the detrended bed elevation and vegetation area ratio

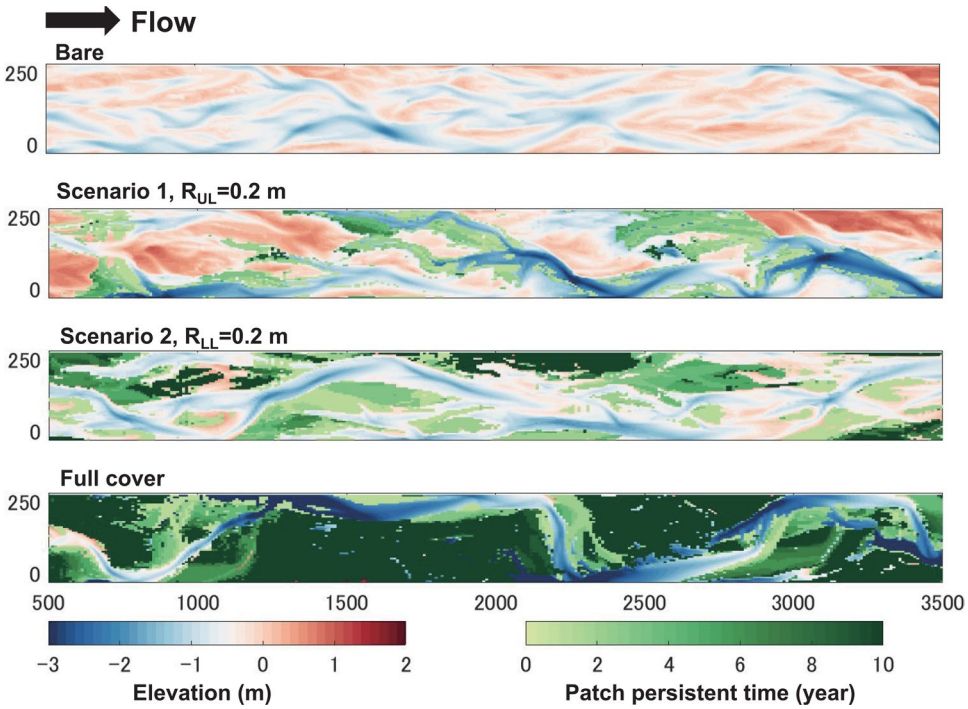

Fig. 4 River morphology and the vegetation distribution for different cases. The patch persistent time indicates the year vegetation keeps its cover at each grid

The braiding index (BI) and the active braiding index (ABI) relative to the vegetation area ratio are provided in Fig. 6. The BI and the ABI were higher for the bare case and lower for the full cover case. In Scenario 1, BI rapidly decreased with a vegetation area ratio increase and approached an equilibrium value until it reached the value of the full cover case. The ABI of Scenario 1 decreased once the vegetation cover ratio was larger than 0.2. With an increase in the vegetation cover ratio, the ABI kept decreasing and there was not an equilibrium value. For Scenario 2, both the BI and the ABI slightly decreased with an increase in vegetation cover, until the vegetation cover ratio was approximately 0.7. If vegetation covered a lower area in Scenario 2 (i.e., a smaller value of R_{LL}), BI and the ABI values rapidly decreased, implying the importance of vegetation growing on a riverbed with lower elevations (the blue arrows in Fig. 6). Compared to Scenario 1, ABI declines more gently for Scenario 2 until the vegetation area ratio reaches approximately 0.7.

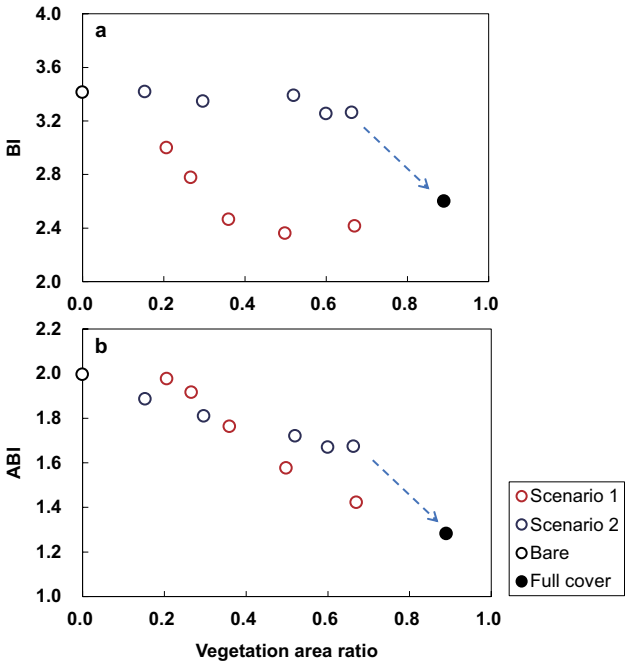

Fig. 6 The braiding index (BI), the active braiding index (ABI), and the vegetation area ratio

Water flow

Wet width, active channel width, and mean water depth (see Sect. "Data analysis" for the definitions) are provided in Fig. 7. Both the wet width and the active channel width decreased with an increase in the vegetation area ratio (Fig. 7a and b). In Scenario 1, the wet width and the active channel width decreased more rapidly than for Scenario 2.

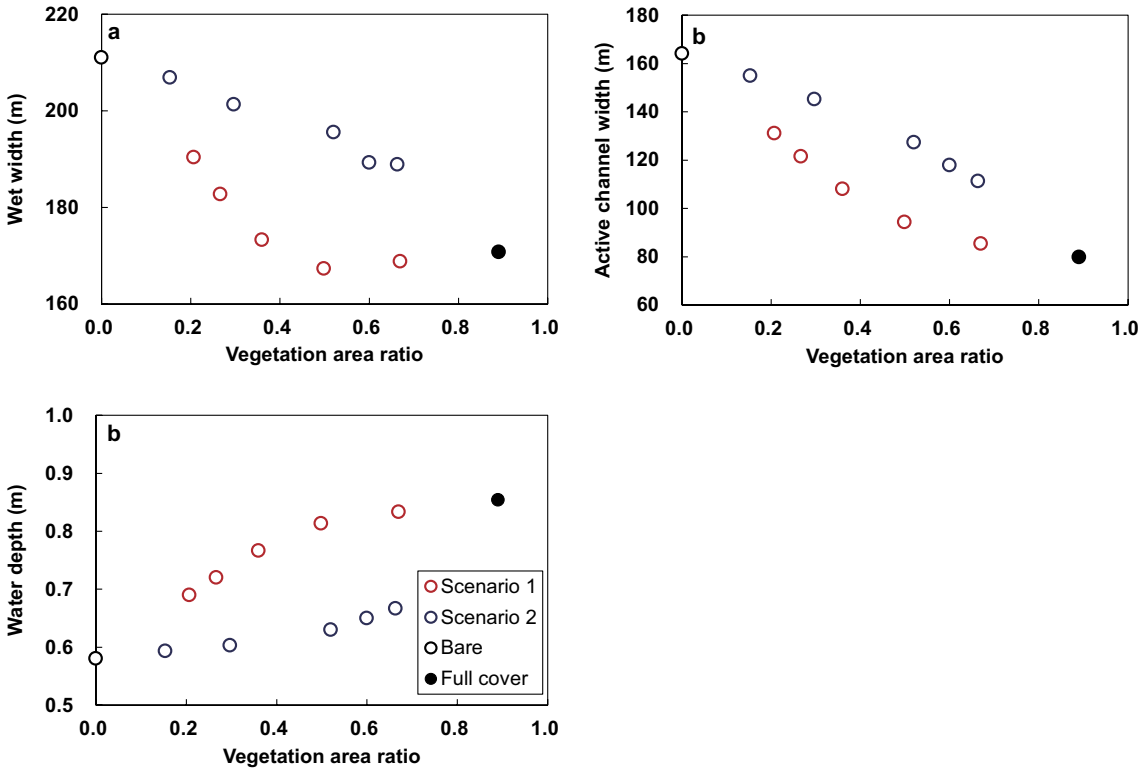

Fig. 7 **a** Wet width, **b** active channel width, and **c** water depth

With a narrowing of channel width due to an increase in the vegetation area ratio, water depth became deeper (Fig. 7c). Similar to channel width, depth increased faster than for Scenario 1 and achieved an equilibrium value at a vegetation area ratio larger than 0.6. For both scenarios, the width of the water surface decreased and the water depth increased with an increase in vegetation area. However, since the P5 elevation did not significantly decrease (Fig. 5), the change in water depth and width in Scenario 2 may have, for the majority of events, resulted from an increase in flow resistance. In Scenario 1, both erosion within the main channel and an increase of flow resistance contributed to an increase of water depth and a decrease in water width.

Flow redirection induced by vegetation

Vegetation in rivers blocks and redirects water flow. The joint histogram of unit discharge and elevation is used to show the effect of vegetation in redirecting water flow. Since it provided a pattern where vegetation blocked small channels and did not cover a large proportion of bar tops (Fig. 8a), the case $R_{UL} = 0.2$ m was selected as the reference case. We compared the bare case to show how vegetation near the water edge affects flow redirection (Fig. 8b). The case $R_{UL} = 1.0$ and the full cover case were compared in order to show the redirecting effect of vegetation in a situation where vegetation covers higher places (Fig. 8c and d). The difference was shown by extracting the joint histogram of the compared cases (Fig. 8b, c and d) from the reference cases (Fig. 8a). The results are, respectively, shown in Fig. 8e, f and g.

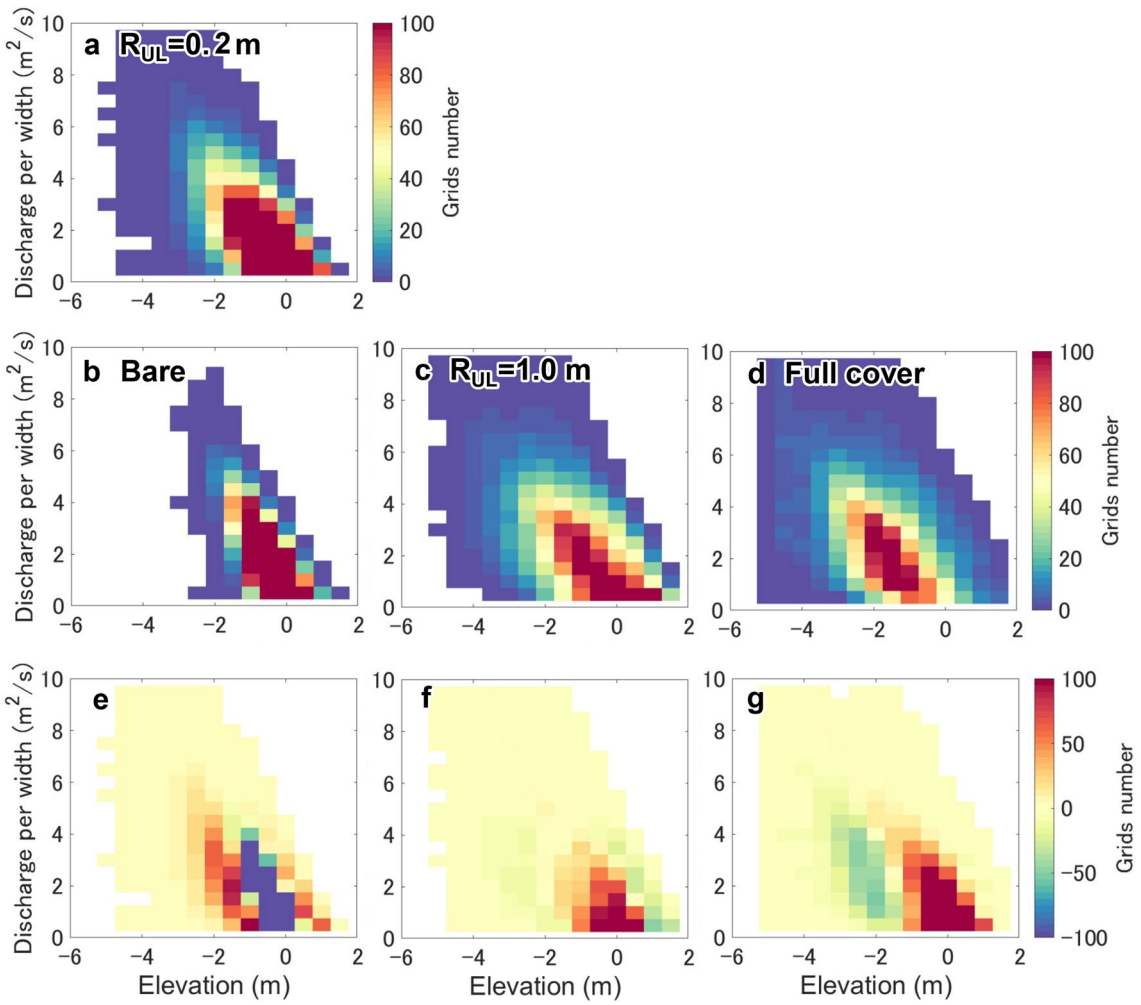

Fig. 8 A joint histogram of discharge per width and elevation. **a** Scenario 1 with $R_{UL} = 0.2$ m. **b** The bare case. **c** Scenario 1 with $R_{UL} = 1.0$ m. **d** The full cover case. **e**, **f** and **g** were obtained by subtracting **b**, **c** and **d** from **a**, respectively. In the histograms, grid number equal to zero is not colored

Figure. 8e indicates that water flow was redirected to low channels and bar tops as compared to the bare case. Since vegetation covered higher places, flow was further redirected to low channels and bar tops (Fig. 8f). When vegetation cover ranged from bar tops to the water's edge, flow was largely concentrated in low channels. The results reveal that vegetation not only redirects flow to low channels, but also to the bar top.

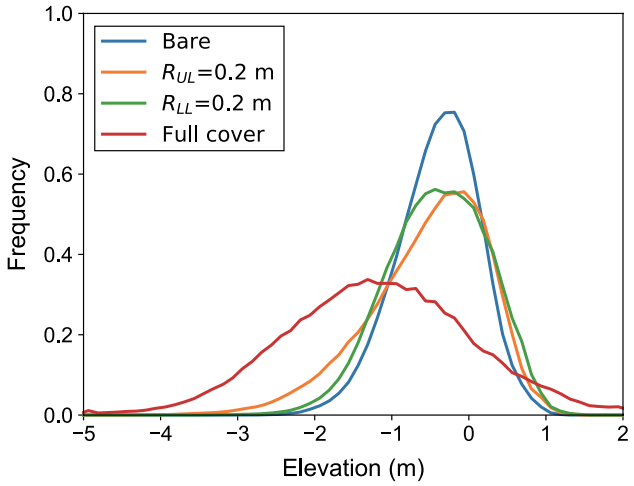

Fig. 9 The distribution of bed elevation for selected cases

Statistical characteristics of the bed elevation distribution

The frequency distribution of bed elevation is provided in Fig. 9. Compared to the bare case, vegetation cover damped the peak of the bed elevation distribution. The peak value of the Full cover case was the smallest. Compared to the case with vegetation cover in high areas (R_{LL} = 0.2 m, the green line), vegetation cover near the water's edge induced more erosion and made the distribution more asymmetrical (R_{UL} = 0.2 m, the orange color line). Vegetation within a high area mainly induces deposition rather than erosion.

The relationship between the statistical characteristics of the bed elevation distribution (i.e., variance, skewness, and kurtosis) and the vegetation area ratio are provided in Fig. 10. The symbol and error bar provide the mean and the standard deviation of the time series for each statistical value. Bed variance increased with an increase in the vegetation area ratio for both scenarios (Fig. 10a). However, the influence of vegetation differed. In Scenario 1, the variance became large for the small vegetation area ratio and

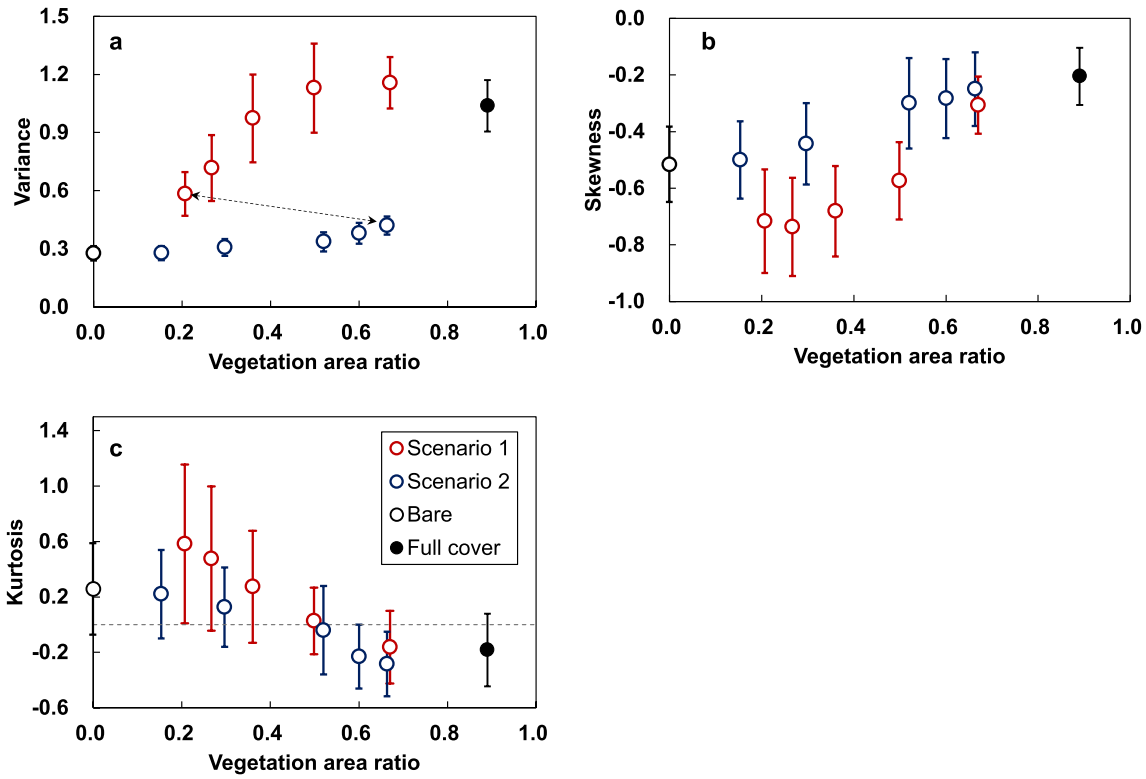

Fig. 10 The relationship between elevation statistical characteristics, **a** elevation variance, **b** elevation skewness, and **c** elevation kurtosis, and the vegetation cover ratio. Error bars represent the standard error of the time series. The arrow indicates a case with R_{UL} = 0.2 m and R_{LL} = 0.2 m. The dashed line in (**c**) indicates a zero value

achieved an equilibrium value for a cover ratio larger than 0.4. In Scenario 2, variance remained almost constant when vegetation cover was less than 0.6 and began to increase with an increase in the vegetation cover ratio when the cover ratio was larger than 0.6. The skewness of bed elevation monotonously increased with vegetation cover in Scenario 2. In Scenario 1, bed skewness for the small vegetation area ratio decreased, and increased for the large vegetation area ratio (Fig. 10b).

The trend for bed kurtosis in Scenario 1 was also not monotonous. Bed kurtosis increased for the small vegetation area ratio and decreased for the large vegetation area ratio (Fig. 10c). In both scenarios, bed elevation displayed a negative skewness and a positive kurtosis for the small vegetation area ratio, and a larger skewness and a negative kurtosis for the large vegetation area ratio.

For Scenario 1, the variance of bed elevation statistical characteristics were larger than for Scenario 2. The results indicate that with a different vegetation distribution, the statistical characteristics of bed elevation in areas subjected to vegetation even varied for the same vegetation cover ratio. Vegetation covering lower areas induced a bed elevation distribution for a larger proportion of the riverbed, with an elevation higher than the cross-sectional mean elevation.

Discussion

A comparison to previous studies

As we mentioned in the Introduction, the change of bed elevation skewness within the Tagliamento River (Bertoldi et al 2011) and the flume experiment (Mao et al. 2020) are different from each other. Mao et al. (2020) attributed the difference between field observations and their flume experiment to a lack of fine sediment within the laboratory experiment. However, as observed for the Tagliamento River, our results for Scenario 2 imply that skewness may increase due to vegetation cover, without the need for fine sediment. Therefore, other factors possibly affected the change of skewness in flume experiments.

For the Tagliamento River study, similar to our Scenario 2, vegetation cover was largely limited to areas with a higher bed elevation. Also, in the Tagliamento River study, bed elevation with less vegetation cover area was more skewed and displayed a positive kurtosis. Skewness became closer to zero and kurtosis became negative with increases in vegetation area. The results obtained for the relationship between skewness, kurtosis, and the vegetation area ratio in Scenario 2 are consistent with field observations. A negatively skewed distribution for cases without vegetation cover was observed in the laboratory experiment performed by Garcia Lugo et al. (2015). However, the change in skewness and kurtosis, together with the vegetation area ratio, was more rapid within the Tagliamento River than within our numerical simulation. A possible reason was that the root reinforcement effect of vegetation was not accounted for in our numerical simulation. With a river bed reinforced by vegetation roots, the bar top was protected; hence, the proportion of higher area relatively increased. Suspended load could be another factor. Since fine sediment can deposit on bar tops, the proportion of low area to high area decreased, which led to an increase in skewness. Other factor effects on the statistical characteristics of the riverbed elevation distribution, such as the reach scale sediment balance and the discharge variability, still require further investigation.

Murray and Paola (2003) proved that with uniformly distributed vegetation a braided river can transform into a single-thread river. Such a tendency was also observed in the laboratory experiment performed by Gran and Paola (2001). The full cover case of our simulation found a consistent tendency with the cellular model and the laboratory experiment. The braiding index (ABI and BI) was larger for Scenario 1 than for the fully covered case. In an early flume experiment (van Dijk et al. 2013), hydrochory vegetation, whose seeds were transported by water flow and the riverbed near water flow, was observed to induce a larger braiding index in river morphology compared to vegetation that was uniformly distributed on the river bed. Thus, Scenario 1 also displayed consistency with the flume experiment. Consistency between the numerical simulation, and the field observations or flume experiments discussed above, supports the view that the numerical model has the potential to reflect morphological changes for braiding rivers with vegetation cover in the field.

Vegetation impacts differ depending on location along a river transect

For both scenarios, the variance of bed elevation is positively related to the vegetation area. Vegetation in low areas has a stronger influence on bed variance than vegetation in high areas (i.e., a relatively small vegetation area can lead to a significant bed variance increase). A large river bed variance indicates that a river has bar tops with relatively high elevations and deep channels. The stronger effect is attributed to the flow concentration induced by vegetation. Since flow was more concentrated by vegetation in Scenario 1, more erosion was induced (e.g., P5 elevation significantly decreased in Scenario 1 (Fig. 5)).

Skewness shows the asymmetry of the bed elevation distribution. A negative skewness indicates that a river has a relatively larger proportion of high area. In Scenario 1 (see the black and red plots in Fig. 10b), since vegetation grew near the water's edge, it induced more erosion in channels rather than deposition on bars when the upper limit of the

habitat was relatively low. The proportion of relatively high area became larger because the mean elevation decreased. Thus, skewness decreased from − 0.52 to − 0.75 with the vegetation area ratio changed from 0 to 0.27. However, the decreasing trend of skewness in Scenario 1 disappeared once the upper limit of the vegetation belt became larger than a critical value ($R_{UL} > 0.2$ m, with a vegetation area ratio larger than 0.27), because vegetation-induced deposition increased the mean elevation and reduced the relative proportion of the high area. In Scenario 2 (see the black and blue plots in Fig. 10b), since deposition on bar tops reduced the relative proportion of a high area, skewness monotonously increased with the vegetation cover ratio. The effect of vegetation in a high area also explains the increasing trend of skewness in Scenario 1. When vegetation covered all of a dry riverbed (the full cover case), the bed elevation distribution was more symmetrical than the bare case. The results suggest that a deep and narrow channel was not a sufficient condition for a skewness reduction.

Bed kurtosis measures the tailedness of a bed elevation distribution. Large kurtosis corresponds to a distribution concentrated at peak and wider tails (the tailedness) as compared with the normal distribution, and a small kurtosis indicates a distribution with a lower peak and narrower tails relative to the normal distribution. Compared to vegetation within the high area, vegetation within the low area induces more erosion, and, therefore, increases the proportion of lower elevation and contributes to an increase in kurtosis. For example, the orange color line in Fig. 9 shows an increased proportion at the lower elevation that contributes to the increased kurtosis of Scenario 1, a small vegetation area ratio (0.2–0.27) can be confirmed in Fig. 10c.

The change in elevation of the river cross sections described in the above paragraphs is depicted within an average cross section using the schematic provided in Fig. 11. The relationship between elevation change and bed statistical properties is indicated in Fig. 11, and the change in bed statistical properties with an increase in the vegetation area ratio is summarized in Table 4.

We also noticed that the full cover case has a larger variance, which cannot simply be explained by adding the effect of vegetation, growing on lower places and on bar tops, on bed variance (e.g., cases indicated by the arrow in Fig. 10a). The results suggest that the combined effect of vegetation on lower places and on bar tops strengthens the influence of vegetation on river morphology. The combined effect can be explained by the flow redirection induced by vegetation. In Scenario 1, although vegetation-induced erosion within

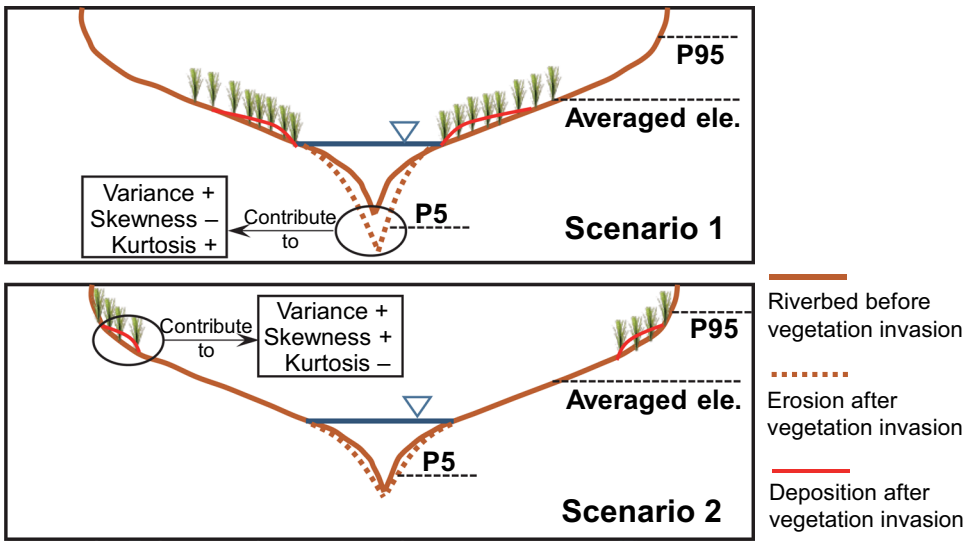

Fig. 11 A schematic showing a change in the averaged river cross section

Table 4 The relationship between bed statistical properties and an increase in the vegetation area ratio

The location of vegetation	Schematic	Bed variance	Bed skewness	Bed kurtosis
Vegetation near the water's edge (Scenario 1)		+ (strong)	–	+
Vegetation on bar tops (Scenario 2)		+ (weak)	+	–

The '+' indicates that the metrics are positively related to the vegetation area increase, and '–' indicates that the metrics are negatively related to the vegetation area increase

the main channel, it also blocked parts of the channels and increased discharge within higher elevations (Fig. 8e and f). If vegetation covered the entire dry bed (e.g., the full cover case), discharge was only concentrated within the main channel without vegetation cover, and more erosion was induced since the width of the main channel was reduced by vegetation.

Discharge deflected by lower elevation vegetation may impact sediment deposition. Deposition that was not proportional to vegetation density (i.e., a less dense vegetation patch with higher sedimentation) was observed in the field. For example, within the Tech River, vegetation located along a transect was found to have different effects on sediment accretion (Corenblit et al. 2009). For the Tech River, neither trees on the bar top nor dense herbs (grass plants) near the low water channel had the largest impact on sediment accretion. However, shrubs between the bar top and the low water channel trapped a larger amount of sediment, and shrub type vegetation displayed a disproportionate importance compared to its abundance (Corenblit et al. 2009, 2020). According to our study, herbs near the low water channel can redirect incoming flow; hence, sediment brought by the flow may contribute to sedimentation in shrubs.

River management focusing on the vegetation transverse distribution

Braided rivers are one of the most dynamic river patterns and support highly dynamic fluvial ecosystems (Tockner et al. 2006). A global trend for a reduction in braided rivers has been reported, and one important reason for this reduction is the expansion of riparian vegetation (Stecca et al. 2019). With conversions from braided rivers to single-thread rivers, the vertical distance between the top of bars and the main channel increases (i.e., an increase in elevation variance), and opportunities for the bar top to be disturbed by flooding are reduced. Under such scenarios, biodiversity may also be reduced since certain species prefer dynamic environments and since these species disappear in stable environments.

One management strategy for recovering morphology and habitat is artificially removing vegetation cover (e.g., tree-cutting (Leu et al. 2008)). Depending on management objectives, different removal methods currently exist. For example, artificially released flushing floods were used to clear vegetation near low water channels (Sumitomo et al. 2018, 2016). The cutting of vegetation on the top of bars may also improve flow capacity during large floods (Toshimori and Miyamoto 2014). Our study indicated that vegetation at different locations along river transects have distinct effects on river morphological development. Therefore, different removal methods for riparian vegetation may lead to different river morphological responses in a vegetated braided river (Fig. 12). Since river morphology is less sensitive to vegetation on high areas, removing vegetation on high areas could be ineffective in recovering a vegetated braided river. Hence, for the originally braided but currently widely vegetated river, removing vegetation near the low water channel or inside a blocked braiding branch is the best strategy for recovery. Since the combined effect between vegetation at

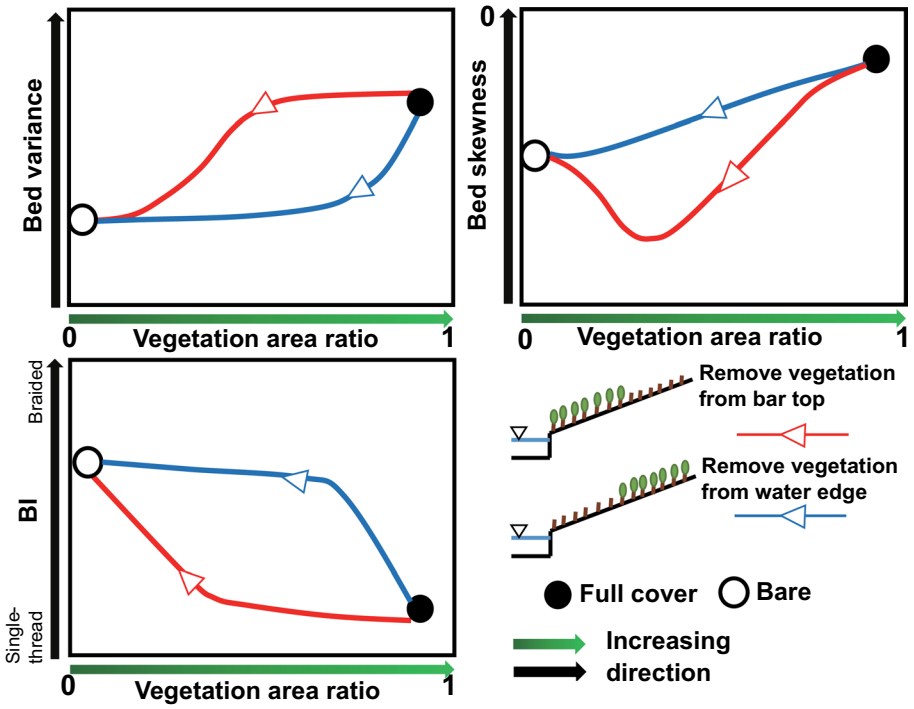

Fig. 12 A schematic figure of two vegetation removal methods and the response of river morphology in an originally braided, but currently vegetated, channel. The horizontal axis provides the vegetation cover ratio. Arrows show the increasing direction

different elevations plays an important role in increasing bed variance, removing vegetation between the bar top and the lower channel may also increase the flow capacity of channels and reduce channel erosion.

In a real river, fine sediment can be deposited within vegetated channels and block channels. Therefore, only removing vegetation may be insufficient for recovering river morphology. Removing vegetation and artificially recovering blocked channels may be a potentially effective management strategy. Such procedures have been used in the past for the Satsunai River in Japan (Sumitomo et al. 2016). However, to date, the long-term effects of such procedures remain unclear. Our study indicates that, from a long-term perspective, such procedures will be effective.

Limits of our results

In our study, we investigated the effects of vegetation distributions along a river transverse on river morphological development. No specific vegetation type was investigated. However, the major parameters of vegetation (density, root depth, and vegetation height) fell within a physical, real range (Jourdain et al. 2020; van Oorschot et al. 2017, 2016; Vargas-Luna et al. 2016). Suspended load was not accounted for in our model. Therefore, our results are more appropriate for a gravel bed river. Vegetation preferences for habitats were not explicitly controlled by physical and ecological processes, and only one type of vegetation was considered. Studying the effects of neglected factors, such as root reinforcement and fine sediment, will be an interesting advancement in our future research.

Our study relied on numerical simulations, which are significantly affected by grid size. Although the large-scale statistics of bar patterns were independent of grid size, the grid resolution in our study may not be fine enough to capture small morphological features on bars (Schuurman and Kleinhans 2011). Numerical studies of the Satsunai River also demonstrated that a grid size of 5 m in the transverse direction can produce results that agree well with field measurements (Sumitomo et al. 2016). Similarly, Iwasaki et al. (2016a, b) used a grid size of 5 m and generated satisfactory results in a river with characteristics comparable to the Satsunai River. Hence, the employed grid resolution is acceptable. However, the impact of such small features on statistical characteristics of the bed elevation distribution is unknown and still requires further investigation.

Conclusions

Using a numerical simulation, we investigated the influence of the transverse vegetation distribution on river morphology development within a braided, gravel bed river. The following scenarios for the transverse vegetation distribution were investigated: (1) vegetation established on the riverbed near the lower channel and (2) vegetation established on the bar top. The numerical model successfully reproduced a reduction in the braiding index within a braided river undergoing vegetation influence. The results indicate that the transverse distribution of vegetation has significantly different effects on river morphology. Vegetation near the water's edge more effectively changes river morphology characteristics, including erosion and the braiding index, and statistical characteristics, as compared to vegetation covering relatively high places. Vegetation near the water's edge not only concentrates flow to major channels within a braided river but also increases discharge on bars by reducing the flow capacity of channels. Based on the different effects of vegetation distribution on river morphology, vegetation management measures in vegetated braided channels can be improved.

Acknowledgements Our study was supported by the Japan Society for the Promotion of Science (JSPS) KAKENHI, grant numbers 20H02257 and 21H01432.

Declarations

Conflict of interest The authors have no competing interests to declare that are relevant to the content of this article.

References

Baar AW, Boechat Albernaz M, van Dijk WM, Kleinhans MG (2019) Critical dependence of morphodynamic models of fluvial and tidal systems on empirical downslope sediment transport. Nat Commun 10:4903. https://doi.org/10.1038/s41467-019-12753-x

Bertoldi W, Gurnell AM, Drake NA (2011) The topographic signature of vegetation development along a braided river: Results of a combined analysis of airborne lidar, color air photographs, and ground measurements. Water Resour Res 47:1–13. https://doi.org/10.1029/2010WR010319

Bertoldi W, Siviglia A, Tettamanti S, Toffolon M, Vetsch D, Francalanci S (2014) Modeling vegetation controls on fluvial morphological trajectories. Geophys Res Lett 41:7167–7175. https://doi.org/10.1002/2014GL061666

Bywater-Reyes S, Diehl RM, Wilcox AC (2018) The influence of a vegetated bar on channel-bend flow dynamics. Earth Surf Dyn 6:487–503. https://doi.org/10.5194/esurf-6-487-2018

Camporeale C, Ridolfi L (2006) Riparian vegetation distribution induced by river flow variability: a stochastic approach. Water Resour Res 42:1–13. https://doi.org/10.1029/2006WR004933

Camporeale C, Perucca E, Ridolfi L, Gurnell AM (2013) Modeling the interactions between river morphodynamics and riparian vegetation. Rev Geophys 51:379–414. https://doi.org/10.1002/rog.20014

Colombini M, Seminara G, Tubino M (1987) Finite-amplitude alternate bars. J Fluid Mech 181:213–232. https://doi.org/10.1017/S0022112087002064

Corenblit D, Steiger J, Gurnell AM, Tabacchi E, Roques L (2009) Control of sediment dynamics by vegetation as a key function driving biogeomorphic succession within fluvial corridors. Earth Surf Process Landf 34:1790–1810. https://doi.org/10.1002/esp.1876

Corenblit D, Vautier F, González E, Steiger J (2020) Formation and dynamics of vegetated fluvial landforms follow the biogeomorphological succession model in a channelized river. Earth Surf Process Landf 45:2020–2035. https://doi.org/10.1002/esp.4863

Crosato A, Saleh MS (2011) Numerical study on the effects of floodplain vegetation on river planform style. Earth Surf Process Landf 36:711–720. https://doi.org/10.1002/esp.2088

Edmaier K, Crouzy B, Perona P (2015) Experimental characterization of vegetation uprooting by flow. J Geophys Res G Biogeosci 120:1812–1824. https://doi.org/10.1002/2014JG002898

Garcia Lugo GA, Bertoldi W, Henshaw AJ, Gurnell AM (2015) The effect of lateral confinement on gravel bed river morphology. Water Resour Res 51:7145–7158. https://doi.org/10.1002/2015WR017081

Gran K, Paola C (2001) Riparian vegetation controls on braided stream dynamics. Water Resour Res 37:3275–3283. https://doi.org/10.1029/2000WR000203

Gurnell A (2014) Plants as river system engineers. Earth Surf Process Landf 39:4–25. https://doi.org/10.1002/esp.3397

Iwasaki T, Shimizu Y, Kimura I (2016a) Numerical simulation of bar and bank erosion in a vegetated floodplain: a case study in the Otofuke River. Adv Water Resour 93:118–134. https://doi.org/10.1016/j.advwatres.2015.02.001

Iwasaki T, Shimizu Y, Kimura I (2016b) Sensitivity of free bar morphology in rivers to secondary flow modeling: Linear stability analysis and numerical simulation. Adv Water Resour 92:57–72. https://doi.org/10.1016/j.advwatres.2016.03.011

Jang CL, Shimizu Y (2007) Vegetation effects on the morphological behavior of alluvial channels. J Hydraul Res 45:763–772. https://doi.org/10.1080/00221686.2007.9521814

Jourdain C, Claude N, Tassi P, Cordier F, Antoine G (2020) Morphodynamics of alternate bars in the presence of riparian vegetation. Earth Surf Process Landf 45:1100–1122. https://doi.org/10.1002/esp.4776

Kang S, Kang H, Ko D, Lee D (2002) Nitrogen removal from a riverine wetland: a field survey and simulation study of Phragmites japonica. Ecol Eng 18:467–475. https://doi.org/10.1016/S0925-8574(01)00107-0

Kim HS, Kimura I, Shimizu Y (2015) Bed morphological changes around a finite patch of vegetation. Earth Surf Process Landf 40:375–388. https://doi.org/10.1002/esp.3639

Lesser GR, Roelvink JA, van Kester JATM, Stelling GS (2004) Development and validation of a three-dimensional morphological model. Coast Eng 51:883–915. https://doi.org/10.1016/j.coastaleng.2004.07.014

Leu JM, Chan HC, Jia Y, He Z, Wang SSY (2008) Cutting management of riparian vegetation by using hydrodynamic model simulations. Adv Water Resour 31:1299–1308. https://doi.org/10.1016/j.advwatres.2008.06.001

Mahoney JM, Rood SB (1998) Streamflow requirements for cottonwood seedling recruitment—an integrative model. Wetlands 18:634–645. https://doi.org/10.1007/BF03161678

Mao, L., Ravazzolo, D., Bertoldi, W., 2020. The role of vegetation and large wood on the topographic characteristics of braided river systems. Geomorphology 367: 107299. https://doi.org/10.1016/j.geomorph.2020.107299

Martínez-Fernández V, Van Oorschot M, De Smit J, González del Tánago M, Buijse AD (2018) Modelling feedbacks between geomorphological and riparian vegetation responses under climate change in a Mediterranean context. Earth Surf Process Landf 43:1825–1835. https://doi.org/10.1002/esp.4356

Millar RG (2000) Influence of bank vegetation on alluvial channel patterns. Water Resour Res 36:1109–1118. https://doi.org/10.1029/1999WR900346

Millar RG (2005) Theoretical regime equations for mobile gravel-bed rivers with stable banks. Geomorphology 64:207–220. https://doi.org/10.1016/j.geomorph.2004.07.001

Mosner E, Weber A, Carambia M, Nilson E, Schmitz U, Zelle B, Donath T, Horchler P (2015) Climate change and floodplain vegetation-future prospects for riparian habitat availability along the Rhine River. Ecol Eng 82:493–511. https://doi.org/10.1016/j.ecoleng.2015.05.013

Murray BA, Paola C (2003) Modelling the effect of vegetation on channel pattern in bedload rivers. Earth Surf Process Landf 28:131–143. https://doi.org/10.1002/esp.428

Nagata T, Watanabe Y, Shimizu Y, INnoue T, Funaki J (2016) Study on dynamics of river channel and vegetation in gravel bed river. J Japan Soc Civil Eng Ser B1 (Hydraulic Engineering) 72:I_1081–I_1086. https://doi.org/10.2208/jscejhe.72.I_1081

Schuurman F, Kleinhans MG (2015) Bar dynamics and bifurcation evolution in a modelled braided sand-bed river. Earth Surf Process Landf 40:1318–1333. https://doi.org/10.1002/esp.3722

Schuurman F, Marra WA, Kleinhans MG (2013) Physics-based modeling of large braided sand-bed rivers: Bar pattern formation, dynamics, and sensitivity. J Geophys Res Earth Surf 118:2509–2527. https://doi.org/10.1002/2013JF002896

Schuurman F, Ta W, Post S, Sokolewicz M, Busnelli M, Kleinhans M (2018) Response of braiding channel morphodynamics to peak discharge changes in the Upper Yellow River. Earth Surf Process Landf 43:1648–1662. https://doi.org/10.1002/esp.4344

Schuurman F, Kleinhans MG (2011) Self-formed braided bar pattern in a numerical model. In: Proceedings of the 5th IAHR Symposium on River, coastal and estuarine morphodynamics, pp 1647–1657.

Solari L, Van Oorschot M, Belletti B, Hendriks D, Rinaldi M, Vargas-Luna A (2016) Advances on modelling Riparian vegetation-hydromorphology interactions. River Res Appl 32:164–178. https://doi.org/10.1002/rra.2910

Stecca G, Zolezzi G, Hicks DM, Surian N (2019) Reduced braiding of rivers in human-modified landscapes: converging trajectories and diversity of causes. Earth Sci Rev 188:291–311. https://doi.org/10.1016/j.earscirev.2018.10.016

Ström L, Jansson R, Nilsson C (2012) Projected changes in plant species richness and extent of riparian vegetation belts as a result of climate-driven hydrological change along the Vindel River in Sweden. Freshw Biol 57:49–60. https://doi.org/10.1111/j.1365-2427.2011.02694.x

Sumi T, Tsunekawa A, Tsujimoto T (2003) A study on physical environment and water-solute transport in surface substrate under vegetation on a sandbar in Kizu River. Adv River Eng 9:389–394

Sumitomo, K., Watanabe, Y., Izumi, N., Yamaguchi, S., Tokohama, H., 2016. Study on the maintenance of former watercourses by the artificial flood for river channel disturbance. J Japan Soc Civil Eng Ser. B1 (Hydraulic Engineering) 72:I_751–I_756. https://doi.org/10.2208/jscejhe.72.I_751

Sumitomo K, Watanabe Y, Izumi N, Yamaguchi S, Yonemoto M (2018) The effect of branched channel maintenance on river channel evolution during floods. J Japan Soc Civil Eng Ser. B1 (Hydraulic

Engineering) 74:I_1003–I_1008. https://doi.org/10.2208/jscejhe.74.5_I_1003

Tal M, Paola C (2007) Dynamic single-thread channels maintained by the interaction of flow and vegetation. Geology 35:347–350. https://doi.org/10.1130/G23260A.1

Tal M, Paola C (2010) Effects of vegetation on channel morphodynamics: results and insights from laboratory experiments. Earth Surf Process Landf 35:1014–1028. https://doi.org/10.1002/esp.1908

Tockner K, Paetzold A, Karaus U, Claret C, Zettel J (2006) Ecology of Braided rivers, in: Braided Rivers. Blackwell Publishing Ltd., Oxford, pp 339–359. https://doi.org/10.1002/9781444304374.ch17

Toshimori N, Miyamoto H (2014) Probabilistic evaluation for flood water level reduction by thinning and cutting-down of a vegetated channel using a vegetation dynamics model. J Japan Soc Civil Eng Ser. B1 (Hydraulic Engineering) 70:I_1381–I_1386. https://doi.org/10.2208/jscejhe.70.i_1381

Tsujimoto T (1999) Fluvial processes in streams with vegetation. J Hydraul Res 37:789–803. https://doi.org/10.1080/00221689909498512

Van Dijk WM, Teske R, Van De Lageweg WI, Kleinhans MG (2013) Effects of vegetation distribution on experimental river channel dynamics. Water Resour Res 49:7558–7574. https://doi.org/10.1002/2013WR013574

van Oorschot M, Kleinhans M, Geerling G, Middelkoop H (2016) Distinct patterns of interaction between vegetation and morphodynamics. Earth Surf Process Landf 41:791–808. https://doi.org/10.1002/esp.3864

van Oorschot M, Kleinhans MG, Geerling GW, Egger G, Leuven RSEW, Middelkoop H (2017) Modeling invasive alien plant species in river systems: interaction with native ecosystem engineers and effects on hydro-morphodynamic processes. Water Resour Res 53:6945–6969. https://doi.org/10.1002/2017WR020854

van Oorschot M, Kleinhans M, Buijse T, Geerling G, Middelkoop H (2018) Combined effects of climate change and dam construction on riverine ecosystems. Ecol Eng 120:329–344. https://doi.org/10.1016/j.ecoleng.2018.05.037

Vargas-Luna A, Crosato A, Calvani G, Uijttewaal WSJ (2016) Representing plants as rigid cylinders in experiments and models. Adv Water Resour 93:205–222. https://doi.org/10.1016/j.advwatres.2015.10.004

Vargas-Luna A, Duró G, Crosato A, Uijttewaal W (2019) Morphological adaptation of river channels to vegetation establishment: a laboratory study. J Geophys Res Earth Surf 124:1981–1995. https://doi.org/10.1029/2018JF004878

Weisscher SAH, Shimizu Y, Kleinhans MG (2019) Upstream perturbation and floodplain formation effects on chute-cutoff-dominated meandering river pattern and dynamics. Earth Surf Process Landf 44:2156–2169. https://doi.org/10.1002/esp.4638

Zong L, Nepf H (2011) Spatial distribution of deposition within a patch of vegetation. Water Resour Res 47:1–12. https://doi.org/10.1029/2010WR009516